Photofragment Translational Spectroscopy of ICl at 304 nm

Kwang-Woo Jung,[†] Temer S. Ahmadi,[‡] and Mostafa A. El-Sayed*

School of Chemistry and Biochemistry, Georgia Institute of Technology, Atlanta, Georgia 30332-0400

Received: March 5, 1997; In Final Form: May 6, 1997[⊗]

The photodissociation dynamics of ICl is studied at 304 nm by state-selective photofragment translational spectroscopy. Velocity distributions, anisotropy parameters, and relative quantum yields are obtained for the ground $I(^2P_{3/2})$ and spin−orbit excited state $I^*(^2P_{1/2})$ iodine atoms, which are produced from photodissociation of ICl at this wavelength. Two sharp velocity distributions are observed for the I channel, suggesting the existence of two dissociation pathways that correlate with ground state iodine formation. Based on the expected translational energy release and the energy separation between those peaks, the two distributions are assigned to dissociation of ICl to $I(^2P_{3/2}) + Cl(^2P_{3/2})$ and to $I(^2P_{3/2}) + Cl^*(^2P_{1/2})$; the former channel appears at higher translational energy. The distribution of I* also shows two strong peaks, indicating that there are two dominant channels for the formation of I* atoms at this wavelength which we assign to the dissociation of ICl forming $I^*(^2P_{1/2}) + Cl(^2P_{3/2})$ and $I^*(^2P_{1/2}) + Cl^*(^2P_{1/2})$, respectively. The quantum yield of $I^*(^2P_{1/2})$ is determined to be 0.30, indicating that the formation of ground state iodine is clearly the favored dissociation channel at 304 nm. The observed anisotropy in the angular distribution of dissociation products (β) indicates that the I* + Cl and I* + Cl* channels are formed predominantly from the parallel transition ($\beta = 1.7$ for both channels) while the I + Cl and I + Cl* products are formed mainly from perpendicular transitions ($\beta = -0.5$). The decrease in the anisotropy parameter of the I formation channels from their limiting value of −1 is attributed to the presence of more than one path for the formation of I + Cl/Cl* photoproducts with opposite polarization for their absorbing transitions. The possible excited state dynamics, which give the observed results, are discussed in terms of the previously proposed energy correlation diagram for ICl.

Introduction

The photodissociation dynamics of diatomic interhalogens have long been the subject of a considerable number of spectroscopic investigations (due to their interesting properties such as predissociation and avoided crossing of potential energy curves).[1−4] The absorption spectrum of gas phase ICl, measured in the wavelength region from 220 to 600 nm,[5] shows two main absorption bands with maxima located at 240 and 470 nm. The extinction coefficients at the maximum for these two bands are 63.7 and 77.0 L/mol cm, respectively.[5] The ICl molecule has four available dissociation pathways which are given below in order of increasing energies of the separate atoms in the product channels. For convenience, $I^*(^2P_{1/2})$ and $Cl^*(^2P_{1/2})$ will be denoted as I* and Cl*, respectively.

$$\begin{aligned} ICl + h\nu &\rightarrow I(^2P_{3/2}) + Cl(^2P_{3/2}) \\ &\rightarrow I(^2P_{3/2}) + Cl^*(^2P_{1/2}) \\ &\rightarrow I^*(^2P_{1/2}) + Cl(^2P_{3/2}) \\ &\rightarrow I^*(^2P_{1/2}) + Cl^*(^2P_{1/2}) \end{aligned}$$

The photodissociation studies of ICl have been carried out in the visible region of 480−530 nm.[6,7] The main oscillator strength is considered to be carried by the bound $B(^3\Pi_{0^+})$ state, which dissociates to form I + Cl*. However, molecular beam studies[7] have shown that both Cl and Cl* atoms are produced from the photodissociation of ICl in this region, with a Cl*/Cl ratio greater than 0.7. The formation of ground state Cl is attributed to predissociation of ICl via an avoided crossing of the bound $B(^3\Pi_{0^+})$ state with a repulsive $Y(0^+)$ state which correlates with the I + Cl channel. There are several experimental studies of this low-energy predissociation process involving determination of curve crossing probabilities and branching ratios of Cl/Cl* formation. These studies include time-resolved laser magnetic resonance,[8,9] Doppler absorption spectroscopy,[10] and photofragmentation spectroscopy.[7]

The early theoretical work on the predissociative channel of ICl was performed by Child and Bernstein[3] using a semiclassical model, who calculated the energy levels of adiabatic states and branching ratios formed by curve crossing. The low-lying potential energy curves, coupling constants, and nonadiabatic coupling effects in the predissociation dynamics of ICl have been studied theoretically.[11,12] Together with the extensive studies in the visible wavelength region, most recent work has focused on vacuum-UV excitation of ICl. These studies dealt with the charge transfer states via fluorescence from vibrational levels of the high-lying energy states $E(0^+)$ and D′ and the strong interaction of Rydberg states with these ion pair states.[13−17] Yencha *et al*. have investigated the vacuum-UV absorption and fluorescence excitation[15] and REMPI spectra[17] of ICl in the 125−195 nm region. They presented evidence for both homogeneous and heterogeneous coupling between $E(0^+)$ ion-pair state and degenerate Rydberg states.[15,17]

In spite of the wealth of spectroscopic[7,13−17] and theoretical[11,12] studies on ICl, detailed information on the photodissociation dynamics of ICl in the UV wavelength region is still very limited both experimentally and theroetically. Recently, Tonokura *et al*.[18] studied the photodissociation of ICl at 235−248 nm by monitoring Doppler profile of REMPI spectra of iodine and chlorine photofragment atoms. They assigned the absorption at this wavelength region to a $^3\Pi_{0^+}$, $^3\Sigma_{0^+}{}^-$, and $^1\Pi_1$

[†] Permanent address: Department of Chemistry, Wonkwang University, Iksan 570-749, Korea.

[‡] Work done in partial fulfillment of Ph.D. requirements from the University of California, Los Angeles.

* To whom correspondence should be addressed.

[⊗] Abstract published in *Advance ACS Abstracts,* July 15, 1997.

S1089-5639(97)00837-2 CCC: $14.00

$\leftarrow {}^1\Sigma_{0^+}{}^-$ transitions leading to the three dissociative channels: I + Cl, I + Cl*, and I* + Cl, indicating that the majority of excited molecules undergoing predissociation via those three states. They noted also the possibility of curve crossing in the exit channel which leads to the observed branching ratios. Recent investigations of the photodissociation of IBr at 304 nm in our laboratory[19] show three dissociation channels: I + Br, I + Br*, and I* + Br with a I* quantum yield of 0.1. The observed anisotropy parameters indicate that these product channels have originated from the $(\sigma^2\pi^3\sigma^{*4}\pi^{*1}) \leftarrow (\sigma^2\pi^4\sigma^{*4}\pi^{*0})$ excitation via parallel or perpendicular transitions: ${}^3\Pi_{0^+}(2341)$, ${}^1\Pi_1(2341)$, and ${}^3\Pi_1(2341)$.

In this article, we use state-selective one-dimensional photofragment translational spectroscopy to investigate the photodissociation of ICl at 304 nm by determining the angular and kinetic energy distributions of the photofragments. The quantum yields for I and I* formation channels are also determined. Such results, along with the measurements of the anisotropy parameter, provide more complete understanding of the correlation between the electronic states and photofragment pathways in this molecule at this wavelength.

Experimental Section

Details of the experimental apparatus and methodology have been described previously.[19,20] Briefly, the gas mixture for the molecular beam is prepared by passing He over ICl sample (*ca.* 10 Torr vapor pressure at room temperature) to make a total pressure of 400 Torr. ICl molecules from a pulsed valve are photodissociated by linearly polarized nanosecond laser pulses to produce iodine and chlorine atoms. Photodissociation experiments are performed at parallel and perpendicular polarization angles with respect to the detection axis, *i.e.*, polarization angles of $\alpha = 0°$ and $\alpha = 90°$, respectively. The iodine atoms, produced in either the ground or spin−orbit excited states, are state selectively ionized within the same laser pulse (304.67 nm for I and 304.02 nm for I* detection). After a delay time of about 2 μs from each laser pulse, the photoions are accelerated toward the detector by applying a pulsed 1 μs acceleration voltage of approximately 1400 V applied to a repelling electrode in the time-of-flight mass spectrometer (TOFMS). The ion packet travels across a second field-free region to a discrimination pinhole (6.0 mm in diameter) placed in front of the detector to reduce the detection solid angle.

ICl (Aldrich, 98% purity) was used without further purification. Prior to use the sample underwent several freeze−pump−thaw cycles, eliminating lower vapor pressure contaminants. The space-charge effect between ionized photofragments is minimized by adjusting the laser power to a maximum of 0.2 mJ/pulse. To ensure that there was no significant I^+ ions produced from multiphoton processes leading to the ionization of ICl then followed by the dissociation of the parent ions, experiments were performed with similar laser power at wavelengths slightly off resonance from the I and I* resonance absorption wavelengths of 304.67 and 304.02 nm. No multiphoton dissociation was observed. It is also necessary to eliminate the interference from clusters since the photofragments from clusters exhibit broader velocity distributions than monomer molecules do.[21,22] Therefore, we have minimized the contribution from clusters by choosing only the early part of the molecular beam pulse for photolysis.

Results

The recoil velocity distributions for production of $I(^2P_{3/2})$ and $I^*(^2P_{1/2})$ at 304.67 and 304.02 nm, respectively, are shown in Figure 1. The peaks at positive and negative velocities correspond to iodine atoms whose initial recoil velocities are toward and away from the detector, respectively. $\alpha = 0°$ and $\alpha = 90°$ indicate parallel and perpendicular polarization of the dissociating laser light with respect to the detection axis. At $\alpha = 0°$ laser polarization angle, the velocity distribution for the formation of I atom shows two peaks of approximately equal intensity located at $v_z = 790$ and 765 m/s (see Figure 1a). This indicates that the I formation channel consists of two different dissociation processes, I + Cl and I + Cl*. The ion signals of these velocity peaks at $\alpha = 90°$ are twice as strong as those at $\alpha = 0°$. The result suggests that the majority of I fragments recoil perpendicular to the direction of the electric vector of the laser light after a photon absorption.

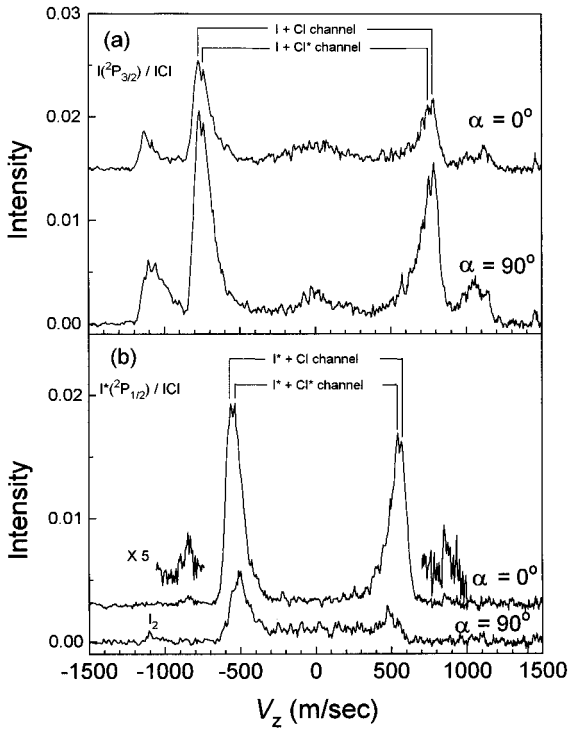

Figure 1. Lab velocity distributions of resonantly ionized (a) ground state and (b) excited state iodine photofragments produced from photodissociation of ICl at 304.67 and 304.02 nm, respectively. The negative and positive velocity peaks correspond to the iodine atoms whose initial recoil velocity is either away from or toward the detector. The notation $\alpha = 0°$ and $\alpha = 90°$ refers to parallel and perpendicular polarization of the electric vector of the dissociating laser with respect to the detection axis. The high-velocity peak ($v_z = 790$ m/s) observed in the spectrum of (a) is assigned to dissociation of ICl to form $I(^2P_{3/2})$ + $Cl(^2P_{3/2})$ while the low-velocity peak ($v_z = 765$ m/s) is assigned to the $I(^2P_{3/2})$ + $Cl^*(^2P_{1/2})$ product channel. The strong peaks at ($v_z =$ 563 and 536 m/s) in (b) are assigned to $I^*(^2P_{1/2})$ + $Cl(^2P_{3/2})$ and $I^*(^2P_{1/2})$ + $Cl^*(^2P_{1/2})$ formation channels. The small peak observed at $v_z \sim$ 1100 m/s in (b) is due to the photodissociation of ICl_3 in the sample.

Figure 1b gives the velocity distributions of iodine ion measured at 304.02 nm, where the excited state iodine atom (I*) can only be selectively ionized. The I* velocity distribution shows also two peaks at $v_z = 563$ and 536 m/s. In contrast to the I formation channel, we were able to detect the relatively small amount of I* atoms only at $\alpha = 0°$. The result provides clear evidence that the I* channel gives a minor contribution in the long wavelength end of the UV absorption band. The intensity difference of I* signals is even greater at the two laser polarization angles as compared with the case of I, indicating that the angular distribution of the I* atom has a strong anisotropic character. In addition, the fact that the ion intensity increases markedly on going from $\alpha = 90°$ to $\alpha = 0°$ is suggestive of a primary photodissociation process with a predominantly parallel polarization dependence.

The two naturally occurring isotopomers of ICl, $^{127}I^{35}Cl$ and $^{127}I^{37}Cl$, have a relative abundance ratio of ~3:1. This means that the recoil velocity distribution of each dissociation channel consists of two components. For I* + Cl* formation channel, for example, the photodissociation of both isotopomers ($^{127}I^{35}Cl \rightarrow {}^{127}I^* + {}^{35}Cl^*$ and $^{127}I^{35}Cl \rightarrow {}^{127}I^* + {}^{37}Cl^*$) can produce the I* atoms. Considering the mass factor, we estimate the difference in the recoil velocity for these two I* components to be $\Delta v_I = 12$ m/s ($\Delta v_{I^*} \propto [\mu(^{127}I^{37}Cl)]^{1/2} - [\mu(^{127}I^{35}Cl)]^{1/2}$, where μ denotes the reduced mass). This small value is due to the existence of two isotopes, excluding the possibility of observing the two peaks with a relative intensity ratio of 3:1. In contrast, the observation of a doublet in the velocity distributions with $\Delta v \sim 30$ m/s clearly demonstrates that these peaks result from the two different dissociation pathways and not from the isotope effect of chlorine atom.

The observation of iodine ion signals having very fast recoil velocities ($v_z = 1120$ and 1060 m/s for I channel and $v_z = 830$ m/s for I* channel) is quite surprising since these components cannot be interpreted in terms of I formation from the photodissociation of ICl molecules. The possibility of these peaks originating from I_2 contamination due to the thermal dissociation of ICl must be considered. The ICl molecule is partially dissociated at room temperature according to the equilibrium $I_2 + Cl_2 \leftrightarrow 2ICl$, $K_{eq} = 3.2 \times 10^5$, giving about 0.2% each I_2 and Cl_2.[23] Iodine atom signals from photodissociation of I_2 impurity would occur at a different recoil velocity, as can be calculated from energy conservation, and thus are easily distinguishable. The small peak observed at $v_z \sim 1100$ m/s for $\alpha = 90°$ (see Figure 1b) is due to the photodissociation of I_2 impurity, which is different from the recoil velocity peaks observed for the pure ICl sample. Furthermore, it has been well-known that photodissociation of I_2 at 304 nm produces stronger I* signal than I signal although the same amount of I and I* atoms are formed after dissociation.[24,25] The very weak signal that appeared in the velocity distribution of I* indicates that there is no detectable contribution from I_2 impurity present in our samples. Therefore, one can notice that the very fast recoil components in I distribution (Figure 1a) have not originated from the I_2 impurities. The presence of Cl_2 molecule does not cause a problem since its photofragment ions are not detected in the present study; *i.e.*, the specific wavelengths for detection are only for iodine fragments.

A possible explanation for high-velocity peaks is due to the fact that small amounts of ICl_3 molecules in the molecular beam can undergo photodissociation (I + Cl + Cl_2 or I + Cl_3) to produce very fast recoiling I/I* atoms as a consequence of the conservation of linear momentum of Cl_3 and I photofragments. This is consistent with our estimation of most probable velocities for the photodissociation of ICl_3, assuming that the C−I bond dissociation energy of ICl_3 is the same as that of ICl molecule. The formation of ICl_3 molecules in the sample could be due to the presence of low-temperature ICl molecules and Cl_2 impurities in the supersonic molecular beam. A possible formation of $ICl\cdots Cl_2$ clusters could produce ICl_3 molecules. Broad velocity distributions of these peaks also support our explanation since the recoil velocity of iodine atoms formed from polyatomic molecules has a broader distribution than that from simple diatomic molecules.

From the measured lab recoil velocity distributions at two different polarization angles, the recoil anisotropy parameters $\beta(v)$ and the recoil speed distributions $G(v)$ can be determined using a deconvolution technique,[20] as shown in Figure 2. The recoil speed distributions of I and I* atoms are narrow, and their maxima have high recoil speeds. Thus, both iodine atoms

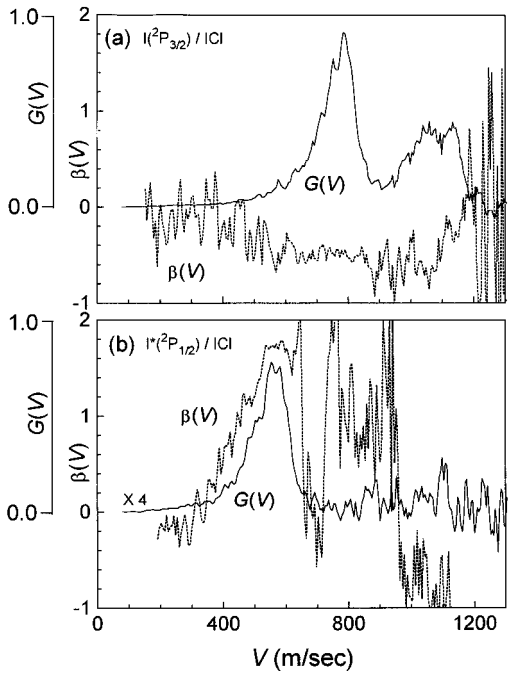

Figure 2. Recoil speed distributions $G(v)$ and the anisotropy parameters $\beta(v)$ of I and I* photodissociation channels obtained from the lab recoil velocity distributions in Figure 1. The intensities of $G(v)$ distributions are normalized in order to show more clearly the polarization dependence. The small peak in $G(v)$ and the large drop in $\beta(v)$ observed at $v = \sim 1100$ m/s for the I* channel (bottom) are due to the photodissociation of I_2.

are produced from repulsive potential energy surfaces which result in nonstatistical translational energy partitioning. The measured ion signal ratio of I* to I is proportional to the branching ratio between I* and I atoms by

$$N(I^*)/N(I) = kS(I^*)/S(I) \quad (1)$$

where S refers to the integrated intensity, obtained from the appropriate $G(v)$ distribution, N is the number of iodine atoms resulting from photodissociation, and k is the proportionality constant. The relative sensitivity ($k = 0.769$) value for detecting I and I* atoms was obtained from the system calibration using I_2 as a standard molecule.[24] The branching ratio, $N(I^*)/N(I)$, of ICl at 304 nm is found to be 0.43. Using the relation between the branching ratio and the relative quantum yields ($\Phi^* = N(I^*)/[N(I^*) + N(I)]$), we obtain $\Phi^* = 0.30$ for the excited state iodine atom. In a recent study on the photodissociation of ICl at 235−248 nm,[18] the branching ratio of $N(I^*)/N(I)$ was determined to be 0.71 using the Doppler absorption spectroscopy. The decrease of I* yield in the present 304 nm wavelength excitation is primarily due to the photon energy dependence of the transitions in the UV absorption band.

The anisotropy parameters $\beta(v)$ of I and I* atoms in Figure 2 provide details to the nature of electronic transitions of the ICl molecule. The angular distributions of the I + Cl and I + Cl* dissociation channels are found to be $\beta = -0.5$, indicating that the perpendicular transition contributes dominantly to these product channels. As Figure 2b shows, for I* + Cl and I* + Cl* channels, β (=1.7) values are close to the limiting value of 2, suggesting that these channels have a strong anisotropic character of parallel transition. The small peak in $G(v)$ and the large drop in $\beta(v)$ observed at $v = \sim 1100$ m/s are due to the photodissociation of I_2.

The use of the correlation between rotational time and anisotropy factor to estimate dissociation time has been treated in our recent studies on C_6H_5I.[26] In this model it is found that

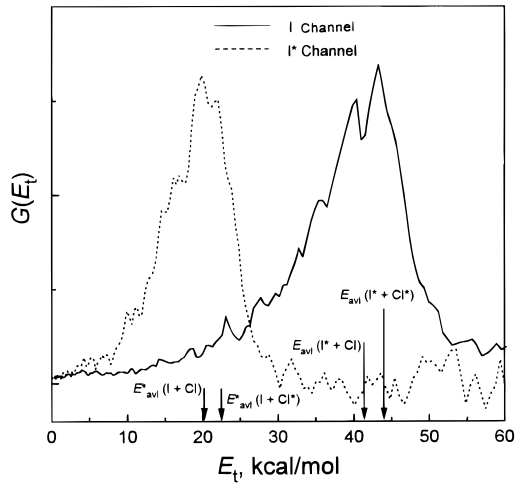

Figure 3. Translational energy release distributions $G(E_t)$ of the I and I* photodissociation channels. The $G(E_t)$ distributions are obtained from the recoil speed distributions in Figure 2 by using an instrumental detection function described in ref 20. The distributions are normalized to the unit peak height.

depolarization is lost purely due to rotation of the molecule during photodissociation and that vibrational excitation whether resulting from thermal excitation or Franck−Condon factor has no significant effect on β value. In the present experiment of ICl photodissociation, the backing pressure for the pulsed valve is kept low (<400 Torr with He gas) to minimize cluster formation in the nozzle expansion. With this stagnation pressure, the temperature of pulse beam is measured to be *ca*. 100 K, which means that ICl molecule in the beam is still rotationally hot. The thermal energy of parent molecule and the instrumental resolution of the TOFMS, which will be described below, contribute to the finite recoil speed distributions of I and I* atoms in the photodissociation of ICl.

Figure 2 shows that the β value for each dissociation channel is independent of recoil speed v. This provides clear evidence that the I and I* atoms produced result from a prompt dissociation in a time scale that is much shorter than the molecular rotation time because of the repulsive nature of the excited states. The assignment of the excited state potentials which give the observed dissociation channels at 304 nm is discussed in detail below. In the case of I* + Cl_3 formation channel, although the ion signal is too weak to give a quantitative β value, they are strong enough to indicate that this channel has also an anisotropic character (parallel transition: $\beta \sim 0.8$ at $v_z = 830$ m/s). On the other hand, we obtain $\beta \sim -0.6$ at $v_z = 1120$ and 1060 m/s for the I + Cl_3 formation channel, which shows also a strong anisotropic character.

The distributions of the total translational energy release, $G(E_t)$, of the I and I* dissociation channels are obtained from their velocity distributions by applying the conservation of linear momentum during the photodissociation process at two recoil angles. E_t is the sum of the translational energies of the iodine and chlorine atoms. These are displayed in Figure 3. The translational energy release distributions, $G(E_t)$, of I and I* atoms have peak widths with fwhm = 12.2 and 10.2 kcal/mol, respectively.

It is obvious that a cold diatomic molecule, excited by a narrow-band laser, will fall apart into a pair of atoms with a single kinetic energy. The finite peak width of the translational energy distribution is ascribed to the (1) thermal energy of the parent molecules, (2) isotope effect of ^{35}Cl and ^{37}Cl atoms, (3) two different dissociation channels, and (4) instrumental resolution of TOFMS. Due to the limitation of applying the high stagnation pressure in order to avoid cluster formation, the parent molecule has its thermal energy of *ca*. 0.5 kcal/mol (∼0.3 and ∼0.2 kcal/mol of translational and rotational energies, respectively; some vibrational excitation could also be present if cooling of the ICl vibration is not complete). The peak broadening due to the isotope effect of ^{35}Cl and ^{37}Cl is calculated to be less than 0.05 kcal/mol, which is negligible in the present measurements. Considering the fact that each distribution consists of two different dissociation channels, *i.e*., I + Cl/Cl* for I formation and I* + Cl/I* for I* formation, the fwhm of translational energy distribution is estimated to be 5−6 kcal/mol for each dissociation channel. This is consistent with our previous results of IBr photodissociation (fwhm = 4−6 kcal/mol for each I + Br, I + Br*, and I* + Br formation channel).[19] Therefore, it is concluded that the major contribution for the peak broadening of translational energy distribution comes from the instrumental resolution of TOFMS due to its single-stage configuration of ion optics.

The available energies E_{avl} and E_{avl}* for I and I* formation channels can be determined from the energy conservation relations:

$$E_{avl}^{(1)} = h\nu - D_0^0(\text{I}-\text{Cl}) + E_{int}^{P} = E_t + E_{int}$$
for the I + Cl formation channel (2)

$$E_{avl}^{(2)} = E_{avl}^{(1)} - E_{SO}(\text{Cl})$$
for the I + Cl* formation channel (3)

$$E_{avl}^{(3)} = E_{avl}^{(1)} - E_{SO}(\text{I})$$
for the I* − Cl formation channel (4)

$$E_{avl}^{(4)} = E_{avl}^{(1)} - E_{SO}(\text{I}) - E_{SO}(\text{Cl})$$
for the I* + Cl* formation channel (5)

where $h\nu$ is the photon energy, D_0^0 the dissociation energy of ICl at 0 K (49.58 kcal/mol),[27] and E_{int}^P the internal energy of the parent molecule. E_{SO}(I) and E_{SO}(Cl) are the spin−orbit excitation energy of iodine (21.74 kcal/mol) and chlorine (2.52 kcal/mol) atoms, respectively. After photodissociation, the available energy partitions into the total translational energy (E_t) of both photofragments since there is no internal excitation, *i.e*., no rotational and vibrational excitation of the atomic iodine and chlorine photofragments ($E_{int} = 0$). E_{int}^P of the parent molecules in the supersonic molecular beam is small and can be neglected in the calculation.

The product state correlation can be directly identified by comparing the observed peak of the translational energy release distribution with the theoretical recoil energy for each dissociation channel. The experimental peak positions are in good agreement with available energies for each dissociation channel (indicated by vertical arrows) in Figure 3. From the calculated and experimental values for E_t we assign the two peaks of the I atom formation to the I($^2P_{3/2}$) + Cl($^2P_{3/2}$) and I($^2P_{3/2}$) + Cl*($^2P_{1/2}$) dissociation pathways. Similarly, the high-energy peak of the I* atom can be assigned to I*($^2P_{1/2}$) + Cl($^2P_{3/2}$) while the low-energy I* peak is assigned to the I*($^2P_{1/2}$) + Cl*($^2P_{1/2}$) channel. The results are summarized in Table 1.

Discussion

The ground state energy configuration of the 10 valence electrons of the ICl molecule is $(\sigma)^2(\pi)^4\ (\pi^*)^4(\sigma^*)^0$, which is abbreviated as (2440). Higher excited states are formed by promotion of one or more electrons from the filled molecular orbitals to the unfilled σ^* orbital, and each state can be well

TABLE 1: Calculated and Experimental Values of E_t for Each Dissociation Channel of ICl

iodine state	λ_{ex} (nm)	$\langle E_t \rangle_{cal}$[b]	$\langle E_t \rangle_{obs}$	product state[c]
I	304.67	44.26	43.39	$I(^2P_{3/2}) + Cl(^2P_{3/2})$
I	304.67	41.74	40.68	$I(^2P_{3/2}) + Cl^*(^2P_{1/2})$
I*	304.02	22.72	22.03	$I^*(^2P_{1/2}) + Cl(^2P_{3/2})$
I*	304.02	20.20	19.97	$I^*(^2P_{1/2}) + Cl^*(^2P_{1/2})$

[a] Energies are in kcal/mol. [b] $\langle E_t \rangle_{cal}$ is obtained by subtracting the dissociation energy D_0^0 (49.58 kcal/mol) of ICl from the experimental energy. [c] The spin−orbit splitting energy for bromine and iodine atoms from *JANAF Thermochemical Tables, J. Phys. Chem. Ref. Data* **1985**, *14* (Suppl. 1).

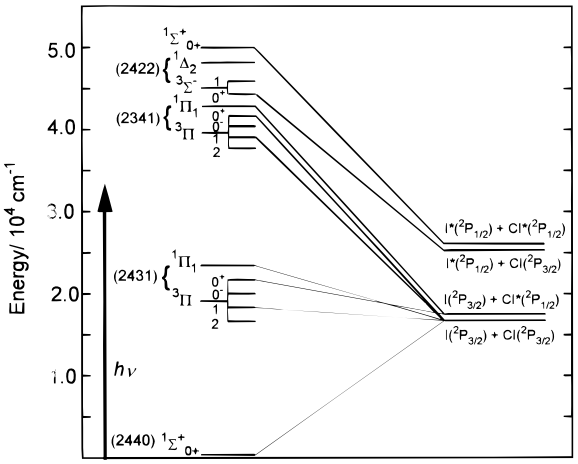

Figure 4. Schematics of energy correlation diagram for the low-lying excited states of ICl based on the results from refs 3, 11, and 12. The vertical arrow indicates photoexcitation of 304 nm wavelength. The dotted curves represent the low-lying excited states that do not contribute to the vertical excitation in the present study due to the high photon energy (4.08 eV) of the photodissociation laser. Numbers in parentheses denote the electronic configuration for each state.

represented by the Hund's case (a) expression. Electronic configurations of ICl are described by term symbols Ω according to spin−orbit couplings where Ω is the projection value of the total electronic angular momentum along the internuclear axis. The parallel transition corresponds to $\Delta\Omega = 0$ and the perpendicular one to $\Delta\Omega = \pm 1$, where $\Delta\Omega$ is the difference between Ω in the upper and lower electronic states. If the dissociation is prompt, the two transitions would give values of β very close to the two limiting values, *i.e.*, $\beta = 2$ for a parallel transition and $\beta = -1$ for a perpendicular transition. Figure 4 shows the schematic correlation energy diagram for several of the low-lying electronic states of ICl molecule responsible for the absorption in the UV and vis region. There are in fact five 0^+ states that correlate with $I(^2P_{3/2}$ or $^2P_{1/2}) + Cl(^2P_{3/2}$ or $^2P_{1/2})$ atoms, two of which correlate with the atomic ground state I + Cl, one with each of the singly excited states I + Cl* and I* + Cl, and one with the same I* + Cl*. The lowest molecular ground state is $X^1\Sigma_{0^+}(2440)$.

The parallel anisotropic character for the I* + Cl and I* + Cl* channels ($\beta = 1.7$ in Figure 2b) suggests that the transition dipole moment lies predominantly parallel to the I−Cl bond axis, and the excited state breaks up on a shorter time scale than a rotational period of the parent molecule. As the ground state for ICl has $\chi^1\Sigma_{0^+}(2440)$ symmetry, the initial transition for this channel must be to an upper state with $\Omega = 0^+$. There are four possible electronic states with $\Omega = 0^+$ that can be reached via a parallel transition: $^1\Sigma_{0^+}{}^+(2422)$, $^3\Sigma_{0^+}{}^-(2422)$, $^3\Pi_{0^+}(2341)$, and $^3\Pi_{0^+}(2431)$. Only $^1\Sigma_{0^+}{}^+(2422)$ and $^3\Sigma_{0^+}{}^-(2422)$ states correlate with the I* + Cl and I* + Cl* products, respectively, in the separated atom limit. Although $^3\Pi_{0^+}(2341)$ correlates adiabatically with I + Cl, it has been reported that there is a curve crossing between the $^3\Pi_{0^+}(2341)$ and $^3\Sigma_{0^+}{}^-(2422)$ states.[18] In this case, the $^3\Pi_{0^+}(2341)$ state correlates diabatically with I + Cl and adiabatically with I* + Cl formation. The curve crossing between these two 0^+ states during dissociation allows an initial transition to either the $^3\Pi_{0^+}(2341)$ or the $^3\Sigma_{0^+}{}^-(2422)$ state resulting in I* + Cl formation. The excitation to the $^3\Sigma_{0^+}{}^-(2422)$ state, however, is a two-electron process and, thus, only weakly allowed. This is consistent with the present observation of less intense signal from I* formation channels than I channels due to the (2422) ← (2440) transition. A similar trend has also been found in the photodissociation of ICl at 235−248 nm,[18] in which the square of the transition moments, μ^2, to the $^3\Pi_{0^+}(2341)$ and $^3\Sigma_{0^+}{}^-(2422)$ states are calculated to be 0.0220 and 0.006 96 $bohr^2$. Therefore, it is most likely that the initial transition is dominantly to the $^3\Pi_{0^+}(2341)$ state followed by curve crossing to the $^3\Sigma_{0^+}{}^-(2422)$ state forming I* + Cl.

The I + Cl and I + Cl* channels are found to have an anisotropy parameter of $\beta = -0.5$ (Figure 2a), suggesting a dominance of perpendicular $\Delta\Omega = \pm 1$ transitions. The observed anisotropy parameters, however, substantially differ from the limiting value, *i.e.*, −1 for the perpendicular transition. This can be explained by proposing that I + Cl and I + Cl* photoproducts originate from a mixed parallel and perpendicular transition. Possible electronic states correlating with I + Cl* product are $^1\Pi_1(2341)$ and $^3\Pi_{0^+}(2431)$. The repulsive wall of a bound state $^3\Pi_{0^+}(2431)$, which correlates also with the I + Cl*, has been considered to be mainly responsible for the absorption band in visible wavelength region (2.2−3.7 eV).[8] In this regard, $^3\Pi_{0^+}(2431)$ state does not contribute to the formation of I + Cl* due to the high photon energy (4.08 eV) in the present study. Thus, we assign the observed I + Cl* channel to be mainly from a direct dissociation of the repulsive $^1\Pi_1(2341)$ state. Since the $^1\Pi_1(2341)$ state does not show any avoided crossing, the perpendicular transition leads adiabatically to I + Cl* products. From measurement of the anisotropy parameter for I_2 photodissociation (which is known to result from a purely perpendicular transition) in our system, we obtain a maximum value of $\beta = -0.90$ (Figure 2b). The observed anisotropy parameter ($\beta = -0.5$) for the I + Cl* channel can be interpreted to result from a considerable contribution of parallel transition. Nonadiabatic curve crossing between repulsive $^3\Pi_{0^+}(2341)$ and bound $^3\Pi_{0^+}(2431)$ states has been well-known in the photodissociation of interhalogen molecules such as ICl and IBr.[3,7] Therefore, it can be concluded that the $^3\Pi_{0^+}(2341)$ transition followed by curve crossing to the $^3\Pi_{0^+}(2431)$ state produces also I + Cl* photoproduct.

The $^3\Pi_{0^+}(2341)$, $^3\Pi_1(2341)$, and $^1\Pi_1(2431)$ states correlate with the I + Cl product channel. The decrease of the anisotropy parameter observed in this channel ($\beta = -0.5$) from its limiting value of −1 can be explained by proposing that I + Cl atoms originate from a mixed parallel and perpendicular transition. Considering the photon energy of photodissociation laser, we can preclude the possibility of the low-lying $^3\Pi_1(2431)$ and $^3\Pi_{0^+}(2431)$ transitions. Therefore, for the perpendicular component of the observed I + Cl dissociation channel, the initial transition would most likely to be the $^3\Pi_1(2341)$ state. The possible assignment for the parallel component is an initial transition to the $^3\Pi_{0^+}(2341)$ repulsive state, which dissociates diabatically into I + Cl. The total results for the assigned excited states of the ICl molecule are presented in Table 2. The low-resolution UV spectra of ICl and IBr are so similar that many of the interpretations discussed above for ICl are considerably consistent with our recent study on IBr.[19]

TABLE 2: Anisotropy Parameter and Assignment for the Dissociation Channels Observed for the Photodissociation of ICl

dissociation channels	λ_{ex} (nm)	β values (obsd)	assignment
$I(^2P_{3/2}) + Cl(^2P_{3/2})$	304.67	−0.5	$^3\Pi_1(2341)$
			$^3\Pi_{0^+}(2341)$
$I(^2P_{3/2}) + Cl^*(^2P_{1/2})$	304.67	−0.5	$^1\Pi_1(2341)$
			$^3\Pi_{0^+}(2341) \rightarrow {}^3\Pi_{0^+}(2431)$
$I^*(^2P_{1/2}) + Cl(^2P_{3/2})$	304.02	1.7	$^3\Pi_{0^+}(2341) \rightarrow {}^3\Sigma_{0^+}{}^-(2422)$
			$^3\Sigma_{0^+}{}^-(2422)$
$I^*(^2P_{1/2}) + Cl^*(^2P_{1/2})$	304.02	1.7	$^1\Sigma_{0^+}{}^+(2422)$

The recoil velocities for I and I* atoms in our photofragment translational spectrometer was calibrated by the signals obtained for I and I* from a well-known standard I_2 molecule.[25] Thus, the dissociation energy of ICl, D_0^0, can be determined from the measured most probable recoil speed by using the energy conservation relations 2−5. We obtain the D_0^0 of ICl to be 50.29 kcal/mol with an estimated uncertainty of less than 0.5 kcal/mol. The dissociation energy from spectroscopic measurements of ICl has been summarized by Evans *et al*.,[23] from which they adopt $D_0^0 = 49.64$ kcal/mol. Calder and Giauque[27] also have reported $D_0^0 = 49.58 \pm 0.03$ kcal/mol using third law analysis. Our result is in good agreement with the previously reported values within 1.5% error.

Acknowledgment. The authors thank the National Science Foundation (Grant CHE9419397) for its financial support of this research. K.-W.J. thanks the Wonkwang University for financial support.

References and Notes

(1) Brooks, W. V. F.; Crawford, B. *J. Chem. Phys*. **1955**, *23*, 363.
(2) Donovan, R. J.; Husain, D. *Trans. Faraday Soc*. **1968**, *64*, 2325.
(3) Child, M. S.; Bernstein, R. B. *J. Chem. Phys*. **1973**, *59*, 5916.
(4) Brand, J. C. D.; Hoy, A. R. *Appl. Spectrosc. Rev*. **1987**, *23*, 285.
(5) Seery, D. J.; Britton, D. J. *J. Phys. Chem*. **1964**, *68*, 2263.
(6) Chichinin, A. I.; Chasovnikov, S. A.; Krasnoperov, L. N. *Chem. Phys. Lett*. **1987**, *138*, 371.
(7) De Vries, M. S.; Van Veen, N. J. A.; Hutchinson, M.; De Vries, A. E. *Chem. Phys*. **1980**, *51*, 159.
(8) Mashnin, T. S.; Chernyshev, A. V.; Krasnoperov, L. N. *Chem. Phys. Lett*. **1993**, *207*, 105.
(9) Chichinin, A. I. *Chem. Phys. Lett*. **1993**, *209*, 459.
(10) Siese, M.; Bässmann, F.; Tiemann, E. *Chem. Phys*. **1985**, *99*, 467.
(11) Balasubramanian, K. *J. Mol. Spectrosc*. **1985**, *110*, 339.
(12) Balasubramanian, K. *Chem. Phys*. **1985**, *95*, 225.
(13) Diegelmann, M.; Hohla, K.; Rebentrost, F.; Kompa, K. L. *J. Chem. Phys*. **1982**, *76*, 1233.
(14) Brand, J. C. D.; Deshpande, U. D.; Hoy, A. R.; Jaywant, S. M. *J. Mol. Spectrosc*. **1990**, *100*, 416.
(15) Lewley, K. P.; Kerr, E. A.; Donovan, R. J.; Hopkirk, A.; Shaw, D.; Yencha, A. J. *J. Phys. Chem*. **1990**, *94*, 6201.
(16) Donovan, R. J.; Lawley, K. P.; Ridley, T.; Wilson, P. J. *Chem. Phys. Lett*. **1993**, *207*, 129.
(17) Donovan, R. J.; Goode, J. G.; Lawley, K. P.; Ridley, T.; Yencha, Y. J. *J. Phys. Chem*. **1994**, *98*, 2236.
(18) Tonokura, K.; Matsumi, Y.; Kawasaki, M.; Kim, H. L.; Yabushita, S.; Fujimura, S.; Saito, K. *J. Chem. Phys*. **1993**, *99*, 3461.
(19) Jung, K.-W.; Griffiths, J. A.; El-Sayed, M. A. *J. Chem. Phys*. **1995**, *103*, 6999.
(20) Hwang, H. J.; Griffiths, J. A.; El-Sayed, M. A. *Int. J. Mass Spectrom. Ion Processes* **1994**, *131*, 265.
(21) Kang, W. K.; Jung, K. W.; Jung, K.-H.; Hwang, H. J. *J. Phys. Chem*. **1994**, *98*, 1525.
(22) Cheng, P. Y.; Zhong, D.; Zewail, A. H. *J. Phys. Chem*. **1995**, *99*, 15733.
(23) Evans, W. H.; Munson, T. R.; Wagmann, D. D. *J. Res. Natl. Bur. Stand*. **1955**, *55*, 147.
(24) Hwang, H. J. Ph.D. Thesis, University of California, Los Angeles, 1991.
(25) Hwang, H. J.; El-Sayed, M. A. *J. Phys. Chem*. **1991**, *95*, 8044.
(26) Hwang, H. J.; El-Sayed, M. A. *J. Chem. Phys*. **1992**, *96*, 856.
(27) Calder, G. V.; Giauque, W. F. *J. Phys. Chem*. **1965**, *69*, 2443.